Advanced Engineering Materials

ADVANCED ENGINEERING MATERIALS
www.aem-journal.com

RESEARCH ARTICLE

Magnetorheological Shear Thickening Polishing Characteristics for Ti-6Al-4V using Multi-Pole Coupling Magnetic Field: A Comprehensive Experimental Study

Yebing Tian | Cheng Qian | Guangyi Wu | Kunal Arora

School of Mechanical Engineering, Shandong University of Technology, Zibo, China

Correspondence: Yebing Tian (tianyb@sdut.edu.cn)

Received: 14 July 2025 | **Revised:** 27 January 2026 | **Accepted:** 27 February 2026

Keywords: magnetorheological shear thickening polishing | material removal rate | polishing force | structural evolution | surface roughness

ABSTRACT

Magnetorheological shear thickening polishing (MRSTP) demonstrates significant potential for the precision processing of titanium alloys. However, prior studies have primarily focused on surface roughness, while comprehensive experimental investigations remain limited. Moreover, the underlying mechanisms have yet to be explored. To address these research gaps, comprehensive MRSTP experiments are conducted on Ti-6Al-4V using a multi-pole coupling magnetic field, considering surface roughness, polishing force, and material removal rate. The optimal parameters are determined, including a carrier fluid concentration of 20 wt%, an abrasive concentration of 7.5 wt%, an abrasive size of 13 μm, a carbonyl iron particle size of 50 μm, a magnetic flux density of 140 mT, a feed rate of 6000 mm/min, and a spindle speed of 100 r/min. After 60 min of MRSTP under these conditions, the surface roughness is reduced from approximately 280 to 24 nm, achieving a mirror-like appearance. The normal and tangential forces are measured to be 4.04 and 1.74 N, respectively, with a corresponding material removal rate of 24.3 mg/h. The formation of enhanced particle clusters explains the underlying mechanisms for these variations. This study provides valuable insights into tailoring MRSTP strategies for specific difficult-to-machine materials and into understanding the MRSTP mechanism.

1 | Introduction

Titanium alloys, particularly Ti-6Al-4V, have attracted significant attention in advanced manufacturing and engineering due to their outstanding corrosion resistance, thermal stability, and excellent biocompatibility [1, 2]. With the continuous expansion of their applications, the demand for superior surface quality has steadily increased [3]. These rising performance requirements underscore the urgent need for advanced polishing technologies that can achieve ultra-smooth surfaces.

Extensive research exists on advanced polishing technologies for Ti-6Al-4V. Li et al. [4] applied laser polishing to Ti-6Al-4V components produced by selective laser melting. Optimizing parameters for both high- and low-power modes reduced surface roughness from Sa 6.38 μm to Sa 1.16 μm. Lee et al. [5] applied laser polishing to an additively manufactured Ti-6Al-4V sample. The reduction in surface roughness led to a significant improvement in fatigue strength and resulted in a smoother surface profile. However, the industrial implementation of laser polishing remains limited due to its high cost and operational complexity. Wang et al. [6] compared shear-thickening polishing, chemical-enhanced shear-thickening polishing, and electrolytic-enhanced shear-thickening polishing for Ti-6Al-4V. All three approaches achieved nanoscale surface quality (~10 nm). However, they inevitably produced a Beilby layer, and its impact on surface integrity requires further investigation. Zhang et al. [7] investigated the electrolytic polishing of Ti-6Al-4V using a chlorine-containing ethylene glycol-based electrolyte. An optimal chloride concentration of 0.4 mol L^{-1} reduced surface roughness by 75.04%. Deng et al. [8] applied chemical-mechanical polishing to Ti-6Al-4V and evaluated the effects of pH and oxidant concentration on the material. The optimal conditions (0.05 wt% H_2O_2

and pH 4) yielded a surface roughness of Ra 1.3 nm. However, both electrolytic and chemical-mechanical polishing involve media that may pose environmental risks.

Currently, magnetic field-assisted polishing technologies demonstrate significant potential for achieving superior surface quality in titanium alloys. Parameswari et al. [9] examined the effects of abrasive particle concentration in magnetorheological fluid and the initial surface roughness of Ti-6Al-4V on finishing performance. Optimization of the fluid composition enabled the achievement of a surface roughness of 95 nm. Rajput et al. [10] developed a feature-based hybrid magnetorheological finishing planning system to mitigate particle settling and instability in magnetorheological fluids. Application of this method resulted in a reduction of the average surface roughness of Ti-6Al-4V bone plates from 324.12 to 21.56 nm. Furthermore, Rajput et al. [11] investigated magnetorheological polishing for biomaterials fabricated by laser cladding. The process yielded a highly polished surface, decreasing R_a from 8.32 to 32.46 nm, and significantly reducing the wear rate from 9.86×10^{-5} mm^3/min to 0.46×10^{-5} mm^3/min. Chen et al. [12] explored the optimal process parameters for the titanium alloy conduit inner using magnetic abrasive finishing. The surface roughness decreased significantly from 0.33 μm to below 0.1 μm. Zhu et al. [13] used spherical composite magnetic abrasive particles to polish a titanium alloy fabricated by selective laser melting. A systematic investigation of the processing parameters resulted in a significant reduction in surface roughness, decreasing from an initial range of 4–10 μm to approximately 100 nm. Recent advancements in polishing media development have further enhanced surface finishing performance. Wang et al. [14] investigated the polishing performance of Fe_3O_4@SiO_2 core–shell magnetic abrasive on TC4 titanium alloy plate. A significant reduction in surface roughness was achieved, from 0.248 to 0.023 μm. Sato et al. [15] developed a high-magnetization magnetorheological finishing media capable of producing ultra-smooth surfaces on aerospace components. After finishing, both planar and freeform surfaces of the Ti-6Al-4V exhibited a mirror-like appearance, indicating excellent surface quality. Rajput et al. [16] proposed a hybrid electrochemical–magnetorheological polishing technique designed to shorten polishing time and enhance the corrosion resistance of Ti-6Al-4V. Under equivalent polishing durations, the hybrid electrochemical–magnetorheological polishing process achieved a 96.4% reduction in surface roughness, compared with only 49.6% for the conventional magnetorheological finishing. The hybrid method reduced the surface roughness of Ti-6Al-4V from 326 to 21.3 nm, while also forming a thick and stable passivation layer. Tien et al. [17] introduced an eco-friendly hybrid chemical magnetorheological fluid, combined with a Halbach array magnetic field, to polish Ti-6Al-4V. Experimental results showed that the optimal oxidant concentration and pH value were 1.5% and 4, respectively. Optimized polishing parameters successfully produced a mirror-like surface finish.

The studies discussed above have primarily contributed valuable insights by exploring and improving polishing media to enhance surface polishing quality. Currently, shear thickening fluids demonstrate significant application potential in the field of ultra-precision machining [18–20]. To combine the advantages of shear thickening fluids and magnetorheological fluids, Tian et al. [21] proposed the magnetorheological shear thickening polishing (MRSTP) method by developing a novel polishing media. This media exhibited dual stimulus responses-shear thickening and magnetization enhancement-which were distinct from the shear thinning behavior of traditional magnetorheological finishing media [22, 23]. A series of polishing experiments on titanium alloy specimens evaluated the technology's performance. Fan et al. [24] polished the planar surface of Ti-6Al-4V using a silicon carbide-based MRSTP media. Surface roughness was reduced significantly from 1.17 μm to a final value of 54 nm. Ma et al. [25] used a cubic boron nitride-enhanced MRSTP media for cylindrical titanium alloy, achieving a reduction in surface roughness from 337.6 to 79 nm. Tian et al. [26] developed an MRSTP bowl-shaped polishing tool. Using cubic boron nitride-based media significantly reduced the surface roughness of the cylindrical titanium alloy from 225 to 42 nm.

Previous studies have primarily concentrated on parameter optimization from the perspective of surface roughness. However, polishing force and material removal rate are also important indicators for evaluating polishing performance. Sidpara et al. [27] investigated the normal and tangential forces in the magnetorheological finishing process. The working gap and magnetic particle concentration were the key parameters influencing polishing force, underscoring the critical role of magnetic field dynamics in determining polishing performance. Ganguly et al. [28] separated the polishing force from other magnetic effects and explored the influence of processing parameters on the polishing force. They found that as the magnetic particle size and working gap increased, both normal and tangential forces decreased, while the feed rate had a relatively minor effect on the tangential force. Kala et al. [29] compared the polishing force characteristics of single-pole and vertically aligned dual-pole magnetic excitation configurations using magnetic abrasive finishing force signals. The dual-pole setup generated a superior normal force, outperforming the single-pole configuration. Liang et al. [30] investigated the planar polishing force characteristics in magnetorheological finishing under a dynamic magnetic field. The polishing force under dynamic conditions was superior to that under a static field. Huang et al. [31] studied the shear force in magnetorheological finishing under a dynamic magnetic field with constant load and variable working gap. Higher constant loads and rotational speeds reduced the working gap and increased the polishing shear force. Although magnetic flux density affected the working gap, its influence on shear force could be neglected.

The material removal rate directly reflects polishing efficiency. Chen et al. [32] used the volume of material removed per unit time to characterize the finishing efficiency of magnetic abrasive finishing on Ti-6Al-4V alloy knee prosthesis. A speed of 1200 r/min resulted in the highest material removal rate. Chen et al. [33] characterized the efficiency of shear-thinning magnetorheological polishing by the material removal depth per unit time. The results showed that this efficiency was most significantly affected by the working gap. Misra et al. [34] evaluated the processing efficiency of ultrasonic-assisted magnetic abrasive finishing based on the amount of material removed per unit time. They found that the material removal rate increased with decreasing working gap and increasing supply voltage. Similarly, Tien et al. [35] applied this method to evaluate the finishing efficiency of magnetorheological finishing on Ti-6Al-4V using enhanced Halbach excitation.

Currently, research on MRSTP has primarily focused on improving the surface quality of Ti-6Al-4V from the perspective of surface roughness. Studies on polishing force and material removal rate have remained confined to theoretical modeling, and the

influence of polishing force on material removal rate remains relatively unexplored [36, 37]. These studies mainly examined the effects of polishing media velocity and magnetic field strength. Additionally, the analysis assumed that surface roughness, polishing force, and material removal rate were independent, and it did not explore the relationships between them. Overall, systematic studies on the wider impacts of MRSTP on titanium alloys are scarce, and the underlying mechanisms responsible for the experimental observations have not yet been elucidated. To clarify the force-MRR-roughness relationship of MRSTP under dual-stimulus responses of magnetization enhancement and shear thickening, and to refine experimental verification and interpretation within the framework of magnetohydrodynamic and particle cluster interaction mechanisms. This study explores the effects of MRSTP media composition and process parameters on surface roughness, polishing force, and material removal rate under a multi-pole coupling magnetic field. The study also revealed the fundamental structural evolution of the MRSTP media composition. This work offers valuable guidance for optimizing the polishing parameters of Ti-6Al-4V and understanding the MRSTP mechanism.

2 | MRSTP Principle

The MRSTP method uses a novel polishing media that responds to both magnetic fields and shear rate. This response forms enhanced particle clusters, which improve surface quality. The polishing media is composed of carbonyl iron particles (CIPs), cubic boron nitride particles (CBNs), fumed silica (SiO_2), and polyethylene glycol (PEG 200). Among these components, SiO_2 and PEG 200 serve as the carrier fluid to provide a shear thickening response, while CIPs contribute to the magnetization enhancement response. Ref. [23] details the supplier information for the polishing media and characterizes its rheological properties under typical operating conditions. The polishing mechanism is shown in Figure 1. Initially, CIPs align along the magnetic lines to form particle clusters under the applied magnetic field. The introduction of relative motion induces the aggregation of SiO_2 and PEG 200, leading to the formation of large agglomerates and micro-convex peaks. This process allows the CBNs to be tightly encapsulated by the agglomerates, resulting in the formation of the enhanced particle clusters. These controlled CBNs within these clusters are pressed into the micro-convex peaks and, assisted by shear action, effectively remove the micro-convex peaks in the form of microchips. Multiple reciprocating cycles gradually smooth the micro-convex peaks to achieve the desired surface quality.

3 | Experimental Details

3.1 | Experimental Setup

The experimental setup was configured on the VKN640 machining center, as depicted in Figure 2. A multi-pole coupling magnetic field polishing tool was attached to the spindle. The magnetic field characteristics of the polishing tool were described in reference [36]. The workpiece was secured to the force plate of the dynamometer using a fixture. The dynamometer was mounted on a vacuum chuck secured to the worktable. The vertical

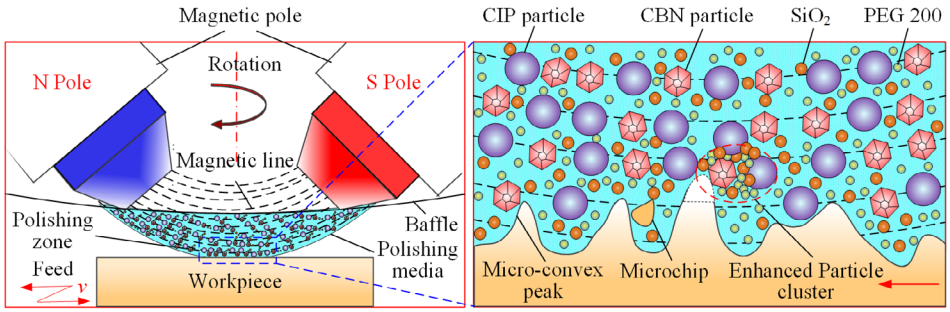

FIGURE 1 | Principle diagram of the MRSTP.

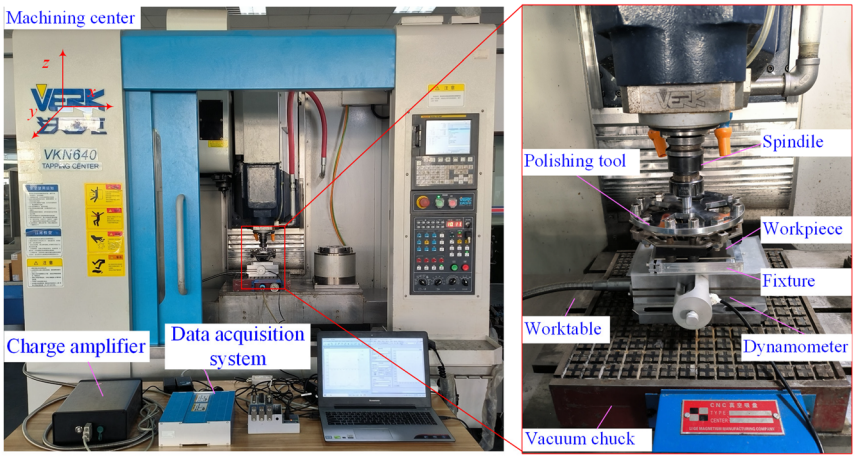

FIGURE 2 | Experimental setup.

movement of the spindle serves as a control mechanism for the magnetic flux density. Meanwhile, the spindle rotation and feed motion of the worktable drove the rotation of the polishing tool and the linear feed of the workpiece, respectively.

3.2 | Experimental Design

Single-factor experiments were performed to systematically evaluate the effects of key variables on surface roughness, polishing force, and material removal rate. Table 1 summarizes the corresponding experimental parameters. A titanium alloy workpiece, measuring 50 mm in length, 20 mm in width, and 2 mm in thickness, was used. Preliminary experiments showed that the surface roughness stabilized after approximately 60 min of polishing, indicating that material removal approached saturation. Thus, the polishing time was set to 60 min, with surface roughness recorded every 10 min for each parameter setting. Upon completion of polishing, data for polishing force and material removal rate were acquired. Each experiment was repeatedly performed three times, and the average value was the final result. The experimental error was quantified using the standard deviation of the three measurements. In cases of significant deviation, the experiment was repeated to ensure the accuracy and reproducibility of the results. The error bars in Figures 3–9 and 11 represent the standard deviation based on the three tests.

4 | Results

4.1 | Influence of Carrier Fluid Concentration

Figure 3 depicts the time-dependent variations in surface roughness, polishing force, and material removal rate as functions of carrier fluid concentration. The results showed that higher carrier fluid concentration led to lower surface roughness but higher polishing force and material removal rate. This phenomenon can be attributed to the enhanced rheological properties of the MRSTP media at higher carrier fluid concentrations, leading to increased viscosity and shear stress [38]. The improved clustering effect within the media promoted the formation of more stable, robust particle clusters, which in turn strengthened the control over abrasion.

4.2 | Influence of Abrasive Concentration

Figure 4 presents surface roughness, polishing force, and material removal rate at different abrasive concentrations. These indicators exhibited no significant variation as the abrasive concentration increased. This effect was primarily attributed to the relatively small variation in abrasive concentration, which consequently had a limited impact on the rheological properties of the MRSTP media. Nevertheless, it caused a moderate increase in the number of active abrasive particles, which slightly reduced the surface roughness while increasing the polishing force and material removal rate.

TABLE 1 | Experiment parameters.

Factor	Level		
Carrier fluid concentration (wt%)	10	15	20
Abrasive concentration (wt%)	3.5	5	7.5
Abrasive particle size (μm)	1.2	3.8	13
Carbonyl iron particle size (μm)	6.5	18	50
Magnetic flux density (mT)	70	100	140
Feed rate (mm/min)	2000	4000	6000
Spindle speed (r/min)	50	100	150

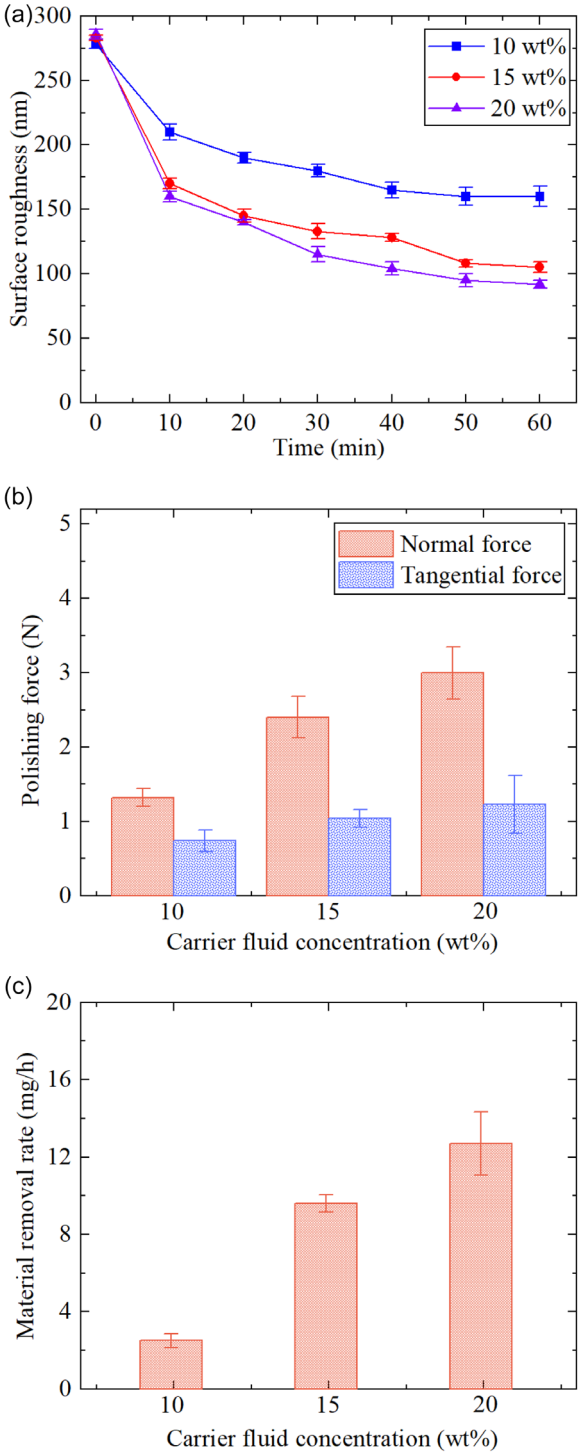

FIGURE 3 | Carrier fluid concentration on various performance parameters. (a) Surface roughness; (b) polishing force; (c) material removal rate.

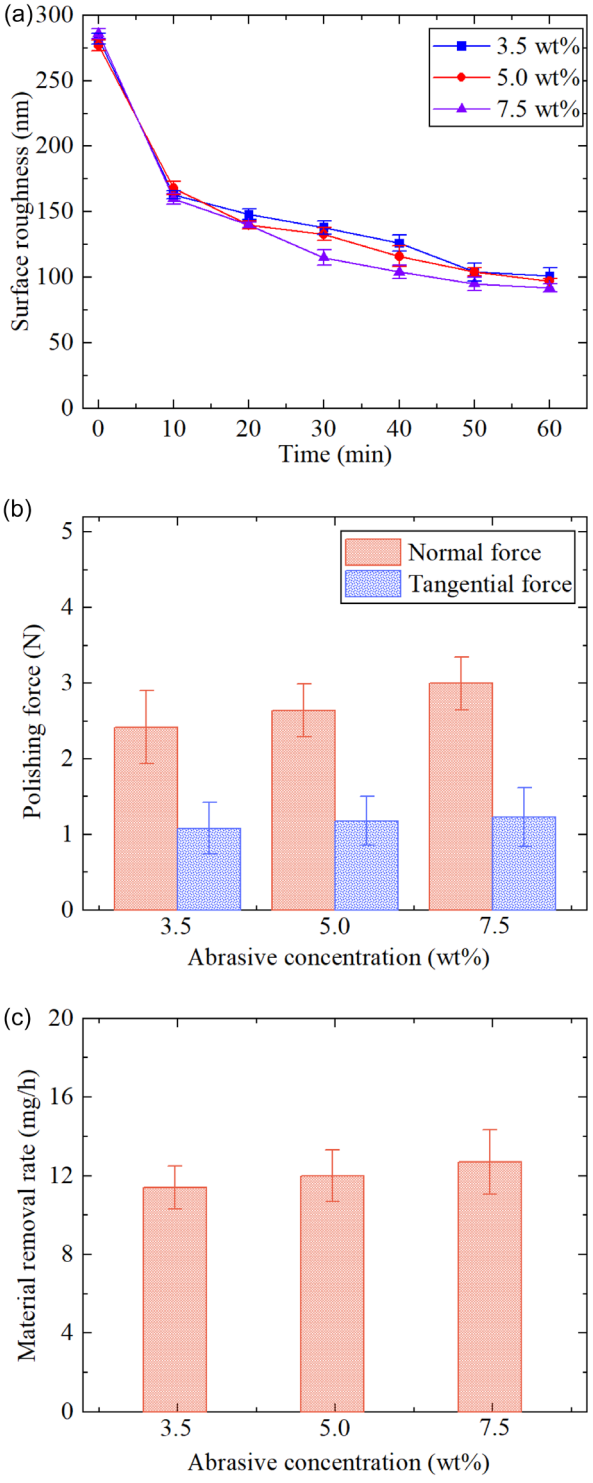

FIGURE 4 | Abrasive concentration on various performance parameters. (a) Surface roughness; (b) polishing force; (c) material removal rate.

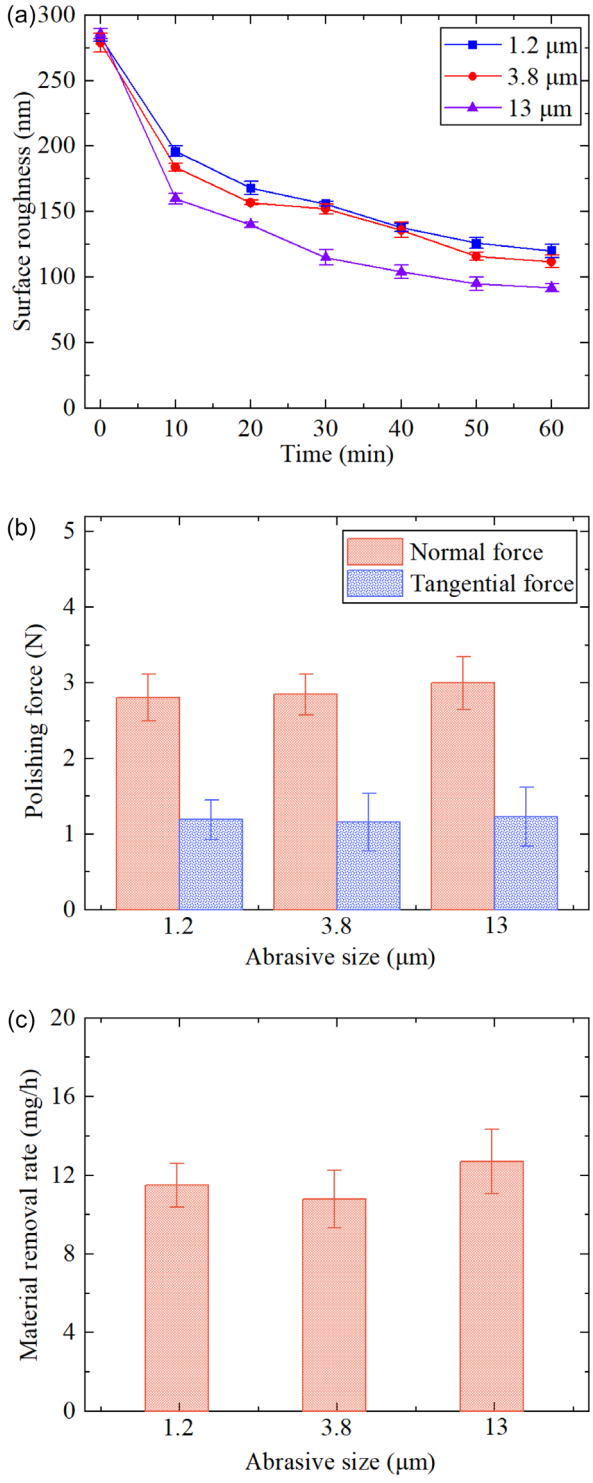

FIGURE 5 | Abrasive particle size on various performance parameters. (a) Surface roughness; (b) polishing force; (c) material removal rate.

4.3 | Influence of Abrasive Particle Size

Figure 5 illustrates the variation in surface roughness, polishing force, and material removal rate with different abrasive particle sizes. As the abrasive particle size increased, these performance indicators showed no significant changes. This effect mainly occurs because the viscosity of the polishing media changes slightly with different abrasive particle sizes. However, the formation range of the enhanced particle clusters expanded to some extent, increasing the content of both dispersed phase and dispersing media. This expansion slightly intensified the clustering effect. Consequently, the stability and strength of the enhanced particle clusters improved moderately, thereby enhancing their capability to control the abrasive particles more effectively.

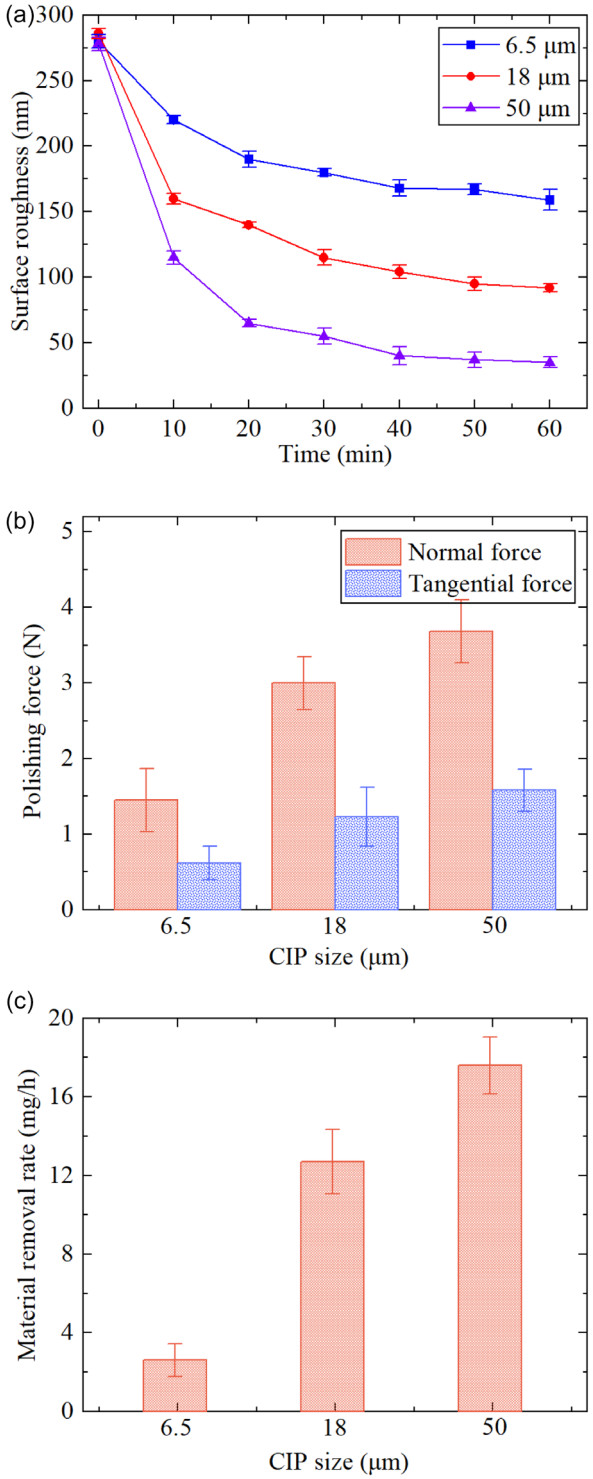

FIGURE 6 | Carbonyl iron particle size on various performance parameters. (a) Surface roughness; (b) polishing force; (c) material removal rate.

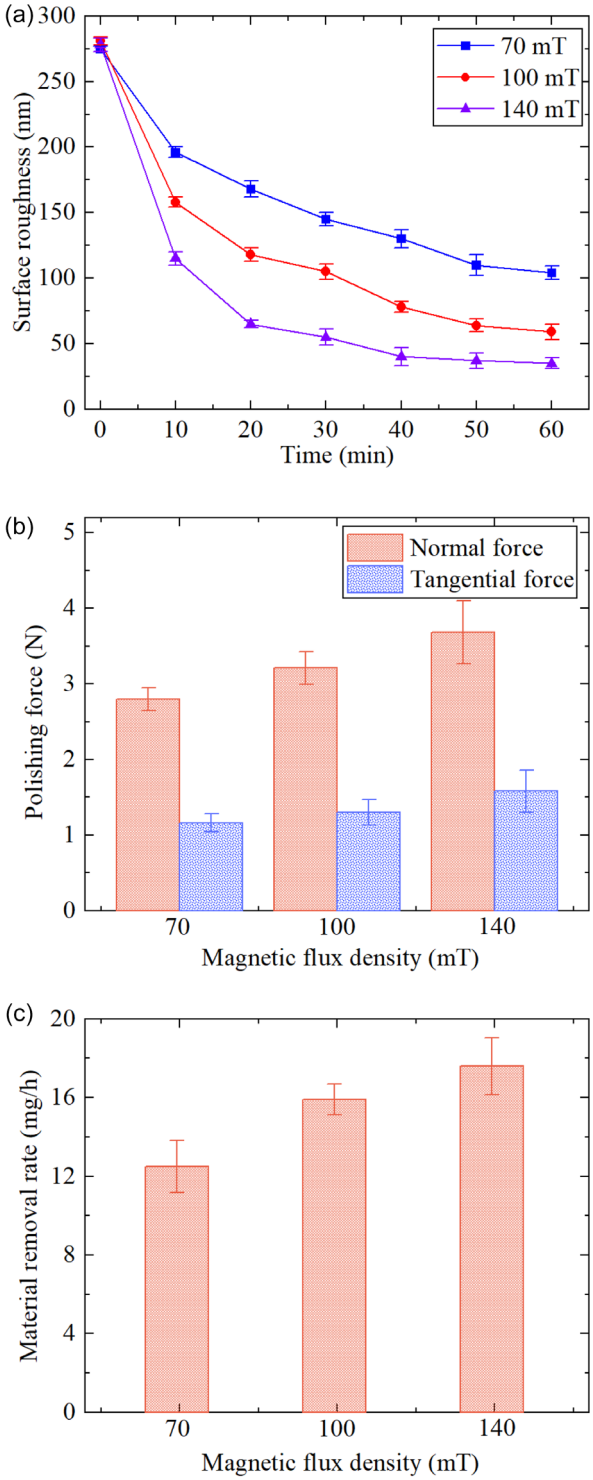

FIGURE 7 | Magnetic flux density on various performance parameters. (a) Surface roughness; (b) polishing force; (c) material removal rate.

4.4 | Influence of Carbonyl Iron Particle Size

Figure 6 demonstrates the significant influence of CIP size on surface roughness, polishing force, and material removal rate, with 50 μm identified as the optimal particle diameter. As the CIP size increased, magnetic dipole interactions between CIPs became stronger, promoting the formation of denser and more stable bundle-like structures of carbonyl iron particles. The intensified magnetic enhancement facilitated the generation of the enhanced particle clusters with greater strength, thereby improving control over abrasive particles.

4.5 | Influence of Magnetic Flux Density

Figure 7 illustrates the variations in surface roughness, polishing force, and material removal rate as the magnetic flux density increases. As the magnetic flux density increased, surface roughness

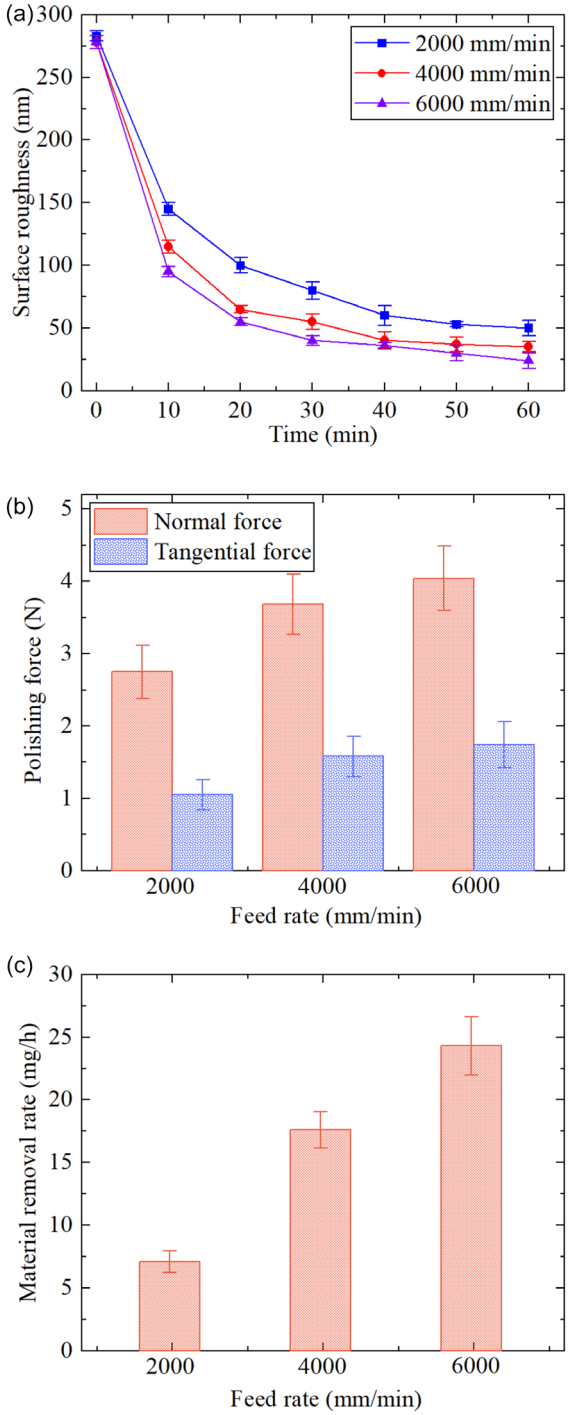

FIGURE 8 | Feed rate on various performance parameters. (a) Surface roughness; (b) polishing force; (c) material removal rate.

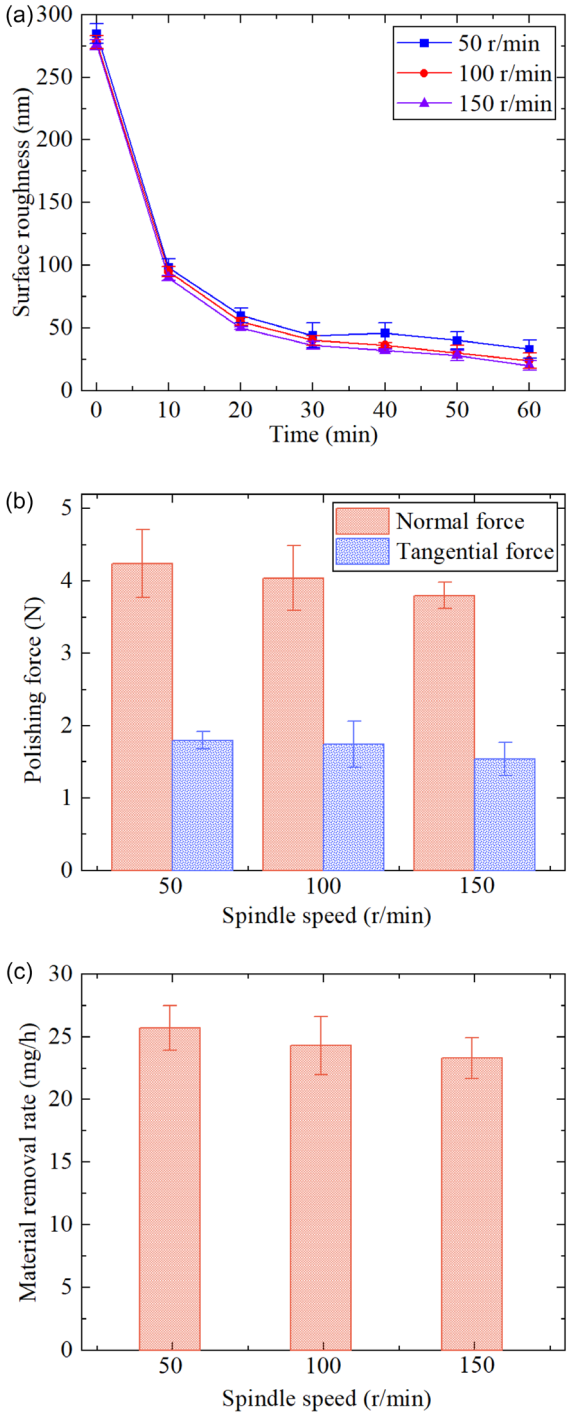

FIGURE 9 | Spindle speed on various performance parameters. (a) Surface roughness; (b) polishing force; (c) material removal rate.

decreased, while polishing force and material removal rate increased. The applied magnetic field imposed a strong directional constraint on the CIPs, promoting the formation of interconnected chain- or bundle-like structures with greater density and stability, thereby significantly reinforcing the enhanced particle clusters.

4.6 | Influence of Feed Rate

Figure 8 presents the time-dependent variations in surface roughness, polishing force, and material removal rate as a function of feed rate. As the feed rate increased, surface roughness exhibited a decreasing trend, whereas both the polishing force and material removal rate increased accordingly. The polishing media experienced a higher shear rate during the MRSTP process, leading to partial disruption or breakage of the chain structures formed by CIP. Nevertheless, the clustering effect between the dispersed phase and the dispersing media was strong enough to preserve the stability and strength of the reinforced particle clusters. Additionally, the increased particle clusters possessed higher kinetic energy. When the encapsulated abrasive

particles came into contact with microscopic surface asperities, their kinetic energy was converted into impact force, effectively removing those asperities. Higher feed rates also intensified the frequency of mechanical interactions (collisions, extrusion, and cutting) between abrasives and the workpiece surface. Overall, both the polishing force and material removal efficiency showed improvement.

4.7 | Influence of Spindle Speed

Figure 9 illustrates the effect of feed rate on surface roughness, polishing force, and material removal rate at increasing spindle speeds. These conditions resulted in a marginal enhancement of surface quality. The refinement of abrasive trajectories contributed to this improvement by reducing surface roughness and increasing polishing uniformity. In contrast, the material removal rate and polishing force steadily declined. The increased spindle speed slightly elevated the movement velocity of the polishing media, resulting in a moderate rise in its kinetic energy. The resultant higher dilution of the polishing media weakened its viscous forces. This thinning effect became dominant. Under the combined influence of these factors, the polishing pressure relatively decreased. The reduction in both normal and tangential force components lowered the penetration depth of individual active abrasive particles, thereby weakening their material removal capability. Although the higher spindle speed increased the frequency of interactions between abrasive particles and surface asperities, this was insufficient to compensate for the negative effects caused by the reduced normal and tangential forces. As a result, the overall material removal rate decreased. An optimal spindle speed of 100 r/min was determined, providing the best balance between surface quality and processing efficiency. The process yielded a surface roughness of 24 nm, with a normal force of 4.04 N, a tangential force of 1.74 N, and a material removal rate of 24.3 mg/h.

4.8 | Surface Morphology

The MRSTP process, under its optimal parameters, produced a significant transformation of the surface morphology, evident in the comparative analysis presented in Figure 10. The initial surface exhibited scratches of various sizes, along with numerous dense and relatively large microscopic peaks. The overall surface quality was relatively rough and lacked mirror-like reflectivity. The MRSTP process successfully eliminated the majority of initial scratches and prominent surface peaks, resulting in a surface with only slight abrasive marks and minor residual impressions. The surface quality was significantly enhanced, exhibiting a mirror-like appearance.

4.9 | Surface Residual Stress

Figure 11 shows the surface residual stress of the workpiece before and after MRSTP. The residual stress changed from an initial tensile stress of 11.8 MPa to a compressive stress of −54.1 MPa. During MRSTP, enhanced particle clusters drive this transition through their action, which includes compression, collision, and impact between the abrasives and the workpiece. These interactions promote plastic deformation, dislocation multiplication, and strain hardening, thereby generating a compressive stress layer. The removal of the shallow, machined-induced tensile stress layer exposes a subsurface region dominated by compressive stress. As MRSTP is a low-temperature finishing process and Ti-6Al-4V does not undergo significant martensitic transformation at room temperature, the observed shift in residual stress is attributed primarily to mechanical effects rather than to thermal stresses or phase transformations. The introduction of compressive residual stress plays a critical role in suppressing crack initiation and propagation, improving fatigue and wear resistance, and ultimately extending the service life of the component.

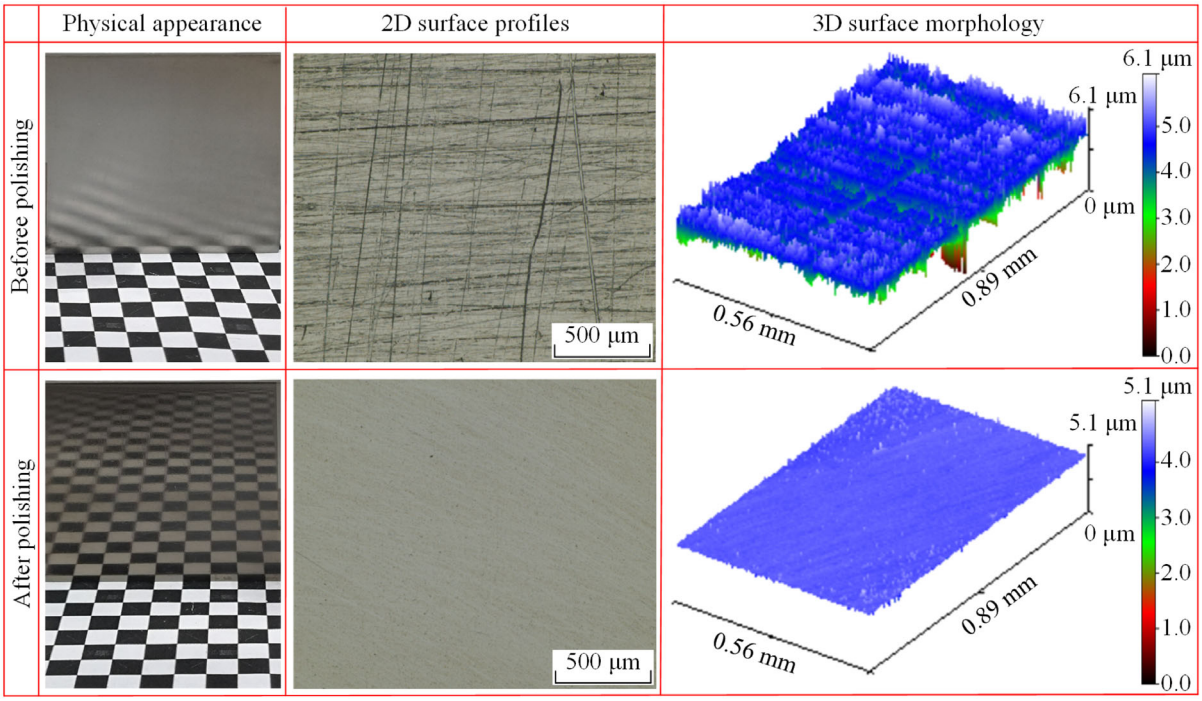

FIGURE 10 | Surface morphologies before and after polishing.

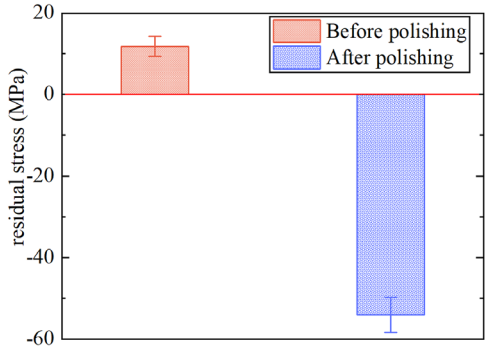

FIGURE 11 | Workpiece surface residual stresses before and after polishing.

5 | Discussion

The above experiments indicated that base fluid concentration, carbonyl iron particle size, magnetic flux density, and feed rate had a significant influence on surface roughness, polishing force, and material removal rate. In contrast, abrasive concentration, abrasive particle size, and spindle speed exhibited a weaker effect on these performance metrics. The microscopic evolution of the MRSTP media components was difficult to observe through experiments [21, 39]. Consequently, the evolutionary characteristics of the enhanced particle clusters were derived from an analysis of rheological behavior, experimental data, and magnetohydrodynamic principles.

During the MRSTP process, the polishing media demonstrated dual stimulus responsiveness, exhibiting both shear-thickening and magnetorheological (or magnetic) enhancement behaviors. The enhanced particle clusters formed due to a combination of the magnetic field, which aligned the CIPs into chain-like structures (Figure 12a), and the clustering interaction between PEG 200 and SiO_2 (Figure 12b). These effects primarily result from the dominance of either shear thickening or magnetization enhancement [23].

Increasing carbonyl iron particle size and magnetic flux density predominantly strengthened the enhanced particle clusters through magnetization enhancement. To facilitate a clearer understanding, we introduce the formula for the magnetic moment of a uniformly magnetized sphere. Based on Equation (1) [40], the magnetic dipole moment of CIPs was directly proportional to the magnetic flux density and the cube of its radius. With increasing CIPs size and magnetic flux density, these chain-like structures tended to aggregate, resulting in thicker and more stable formations [41]. This structural evolution increased the hindrance to SiO_2 aggregation, thereby weakening the shear thickening behavior [42]. The strengthened enhanced particle clusters shown in Figure 12c,d exhibit a greater ability to regulate abrasive particles compared to those in Figure 12b. This improvement facilitated more effective removal of microscopic surface asperities.

$$m = \frac{4B}{3\mu_0}\pi r_f^3 \chi \tag{1}$$

where m is magnetic dipole, B is the strengthen of magnetic flux density, μ_0 is vacuum permeability, r_f is radius of CIP and χ is the magnetic permeability of CIP.

The shear thickening effect further contributed to the strength of the enhanced particle clusters. The effect reflected the degree of integration between SiO_2 and PEG 200. According to the rheological analysis, the structural composition of the MRSTP media under a magnetic field conformed to a body-centered cubic arrangement [23, 43]. As

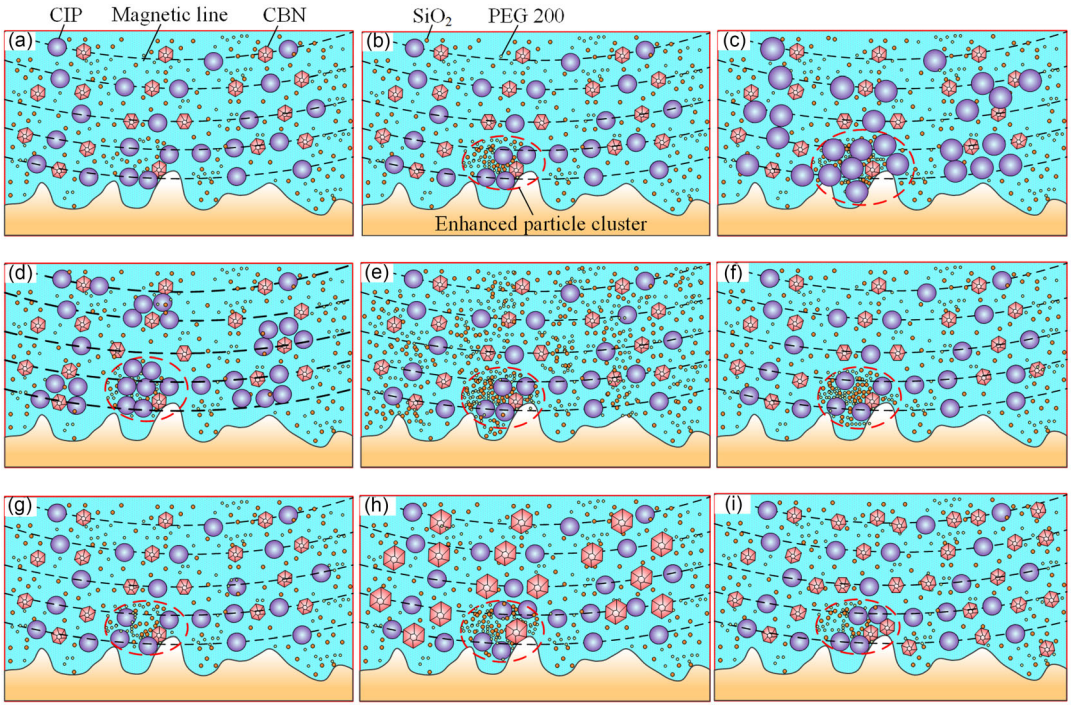

FIGURE 12 | Structural evolution characteristics of the enhanced particle clusters under various parameters. (a) Apply a magnetic field; (b) shear rate; (c) increased carbonyl iron particles size; (d) increased magnetic flux density; (e) increased carrier fluid concentration; (f) increased feed rate; (g) increased spindle speed; (h) increased abrasive particle size; (i) increased abrasive concentration.

the carrier fluid concentration increased, the likelihood of interaction between SiO_2 and PEG 200 rose, thereby amplifying the clustering effect within the MRSTP media, as shown in Figure 12e [38]. With an increase in feed rate, short-range hydrodynamic lubrication force facilitated the secondary aggregation of SiO_2 clusters, resulting in the formation of a more stable enhanced particle cluster (Figure 12f). During this phase, the magnetohydrodynamic pressure acting on the directionally enhanced particle clusters intensified. In contrast, although a higher spindle speed slightly elevated the movement velocity of the polishing media, the reduction in viscous force became the dominant factor. Consequently, the corresponding enhanced particle clusters weakened (Figure 12g). Nevertheless, the increased spindle speed contributed to the refinement of abrasive motion trajectories, which improved surface quality to a certain extent. An increase in abrasive particle size enlarged the particle dimensions, creating more residual space within the enhanced particle clusters. This confined space accommodated more SiO_2 and PEG 200, but not enough to significantly affect the rheological properties [23]. Therefore, this behavior slightly enhanced the clustering effect, as shown in Figure 12h. Increasing the abrasive concentration caused a slight reduction in the relative proportion of the carrier fluid. However, due to the limited range of this increase, its impact on the clustering effect remained negligible. The number of active abrasive particles involved in the enhanced particle cluster increased, as shown in Figure 12i.

6 | Conclusions

The work conducted comprehensive MRSTP experiments on Ti-6Al-4V using a multi-pole coupling magnetic field, focusing on the surface roughness, polishing force, and material removal rate. The analysis was extended to characterize the structural evolution of the polishing media under various parameters. The main conclusions were as follows:

(1) Single-factor experiments revealed that base fluid concentration, CIP size, magnetic flux density, and feed rate had a significant influence on surface roughness, polishing force, and material removal rate. Additionally, a moderate increase in spindle speed was beneficial for achieving a high-quality surface.

(2) The optimal surface roughness was significantly reduced from approximately 280 to 24 nm, effectively eliminating the original surface scratches. The corresponding normal and tangential forces were 4.04 N and 1.74 N, respectively, and the material removal rate reached 24.3 mg/h.

(3) The improvement in surface quality was attributed to the influence of polishing media components and processing parameters on shear thickening and magnetization enhancement, thereby altering the degree of formation of the enhanced particle clusters.

Author Contributions

Yebing Tian: conceptualization, methodology, funding acquisition, project administration, resources, supervision, writing – review & editing. **Cheng Qian**: investigation, conceptualization, methodology, visualization, writing – original draft. **Guangyi Wu**: investigation, methodology, writing – review & editing. **Kunal Arora**: investigation, writing – review & editing.

Acknowledgments

The authors gratefully acknowledge financial supports by Shandong Provincial Natural Science Foundation, China (Grant No. ZR2023ME112), Taishan Scholar Special Foundation of Shandong Province (Grant Nos. tstp20240826 and tsqn201812064), and Key Research and Development Project of the Ningxia Hui Autonomous Region (No. 2024BEE02019).

Funding

This study was supported by Shandong Provincial Natural Science Foundation, China (Grant ZR2023ME112), Taishan Scholar Special Foundation of Shandong Province (Grant tstp20240826 and tsqn201812064), Key Research and Development Project of the Ningxia Hui Autonomous Region (Grant 2024BEE02019), and National Natural Science Foundation of China (Grant 52575516).

Conflicts of Interest

The authors declare no conflicts of interest.

Data Availability Statement

The data that support the findings of this study are available from the corresponding author upon reasonable request.

References

1. E. Abd-Elaziem, M. A. Darwish, A. Hamada, and W. M. Daoush, "Titanium-Based Alloys and Composites for Orthopedic Implants Applications: A Comprehensive Review," *Materials & Design* 241 (2024): 112850.

2. L. C. Zhang and L. Y. Chen, "A Review on Biomedical Titanium Alloys: Recent Progress and Prospect," *Advanced Engineering Materials* 21 (2019): 1801215.

3. M. Najafizadeh, S. Yazdi, M. Bozorg, et al., "Classification and Applications of Titanium and Its Alloys: A Review," *Journal of Alloys and Compounds Communications* 3 (2024): 100019.

4. J. J. Li, H. Y. Wu, H. X. Liu, and D. W. Zou, "Surface and Property Characterization of Selective Laser-Melted Ti-6Al-4V Alloy after Laser Polishing," *The International Journal, Advanced Manufacturing Technology* 128, no. 1 (2023): 703–714.

5. S. J. Lee, Z. Ahmadi, J. W. Pegues, M. Mahjouri-Samani, and N. Shamsaei, "Laser Polishing for Improving Fatigue Performance of Additive Manufactured Ti-6Al-4V Parts," *Optics and Laser Technology* 134 (2021): 106639.

6. J. H.Wang, Y. Zhou, Z. Qiao, et al., "Surface Polishing and Modification of Ti-6Al-4V Alloy by Shear Thickening Polishing," *Surface & Coatings Technology* 468 (2023): 129771.

7. Y. F. Zhang, J. Z. Li, S. H. Che, and Y. W. Tian, "Electrochemical Polishing of Additively Manufactured Ti–6Al–4V Alloy," *Metals and Materials International* 26, no. 6 (2020): 783–792.

8. C. B. Deng, L. Jiang, N. Qin, and L. M. Qian, "Effects of pH and H2O2 on the Chemical Mechanical Polishing of Titanium Alloys," *Journal of Materials Processing Technology* 295 (2021): 117204.

9. G. Parameswari, V. K. Jain, J. Ramkumar, and L. Nagdeve, "Experimental Investigations into Nanofinishing of Ti6Al4V Flat Disc Using Magnetorheological Finishing Process," *The International Journal, Advanced Manufacturing Technology* 100 (2019): 1055.

10. A. S. Rajput, M. Das, and S. Kapil, "Surface Properties and Biocompatibility Studies on Bone Plate by the Magnetorheological Finishing (MRF) Process," *Surface Engineering* 38, no. 7–9 (2022): 797–806.

11. A. S. Rajput, M. Das, and S. Kapil, "Investigation of Surface Characteristics on Post Processed Additively Manufactured Biomaterial through Magnetorheological Fluid Assisted Finishing Process," *Wear* 522 (2023): 204684.

12. Y. Chen, L. B. Li, J. H. Zeng, L. Kang, and B. Han, "Experimental Study on Precision Grinding of Titanium Alloy Conduit Inner Surface in Aero-Engine," *Aerospace Manufacturing Technology* 61 (2018): 40.

13. P. X. Zhu, G. X. Zhang, X. Teng, J. J. Du, L. Z. Jiang, and H. X. Chen, "Investigation and Process Optimization for Magnetic Abrasive Finishing Additive Manufacturing Samples with Different Forming Angles," *The International Journal, Advanced Manufacturing Technology* 118 (2022): 2355.

14. Y. L. Wang, Y. T. Kang, W. J. Zhang, and X. C. Yin, "Synthesis and Characterization of Fe3O4@SiO2 Core-Shell Nanoparticles for Mirror and Efficient Magnetic Compound Fluid Polishing of TC4 Titanium Alloy," *Surface Topography: Metrology and Properties* 12 (2024): 035041.

15. T. Sato, C. W. Kum, and V. C. Venkatesh, "Rapid Magneto-Rheological Finishing of Ti-6Al-4V for Aerospace Components," *International Journal of Nanomanufacturing* 9 (2013): 431.

16. A. S. Rajput, M. Das, and S. Kapil, "A Hybrid Electrochemical Magnetorheological Finishing Process for Surface Enhancement of Biomedical Implants," *Journal of Manufacturing Science and Engineering* 146, no. 5 (2024): 051004.

17. D. H. Tien and N. D. Trinh, "Novel Hybrid Chemical Magnetorheological Fluid for Polishing Ti–6Al–4V Alloy," *Materials and Manufacturing Processes* 39 (2024): 1798.

18. X. Y. Chen, J. Y. Cai, L. Y. Shao, and B. H. Lyu, "Parameters Optimization of Active Flexible Tool-Assisted Shear Thickening Polishing Method for Concave Surface," *Advanced Engineering Materials* 26 (2024): 2400366.

19. X. Wang, Z. Y. Bao, J. H. Wang, et al., "Optimization Study of Shear-Thickening Polishing Technology in the Passivation Process of Spiral-Fluted Tap Edge Based on Simulation Analysis," *Advanced Engineering Materials* 27 (2025): 2402476.

20. B. C. Sun, Z. X. Wang, Y. Zhao, et al., "Research Progress of Shear-Thickening Polishing Technology: A Review," *Precision Engineering* 95 (2025): 322.

21. Y. B. Tian and Z. H. Z.H.Fan, *Ultra-Precision Magnetorheological Shear Thickening Finishing* (Science Press, 2022).

22. M. Kumar, A. Kumar, R. K. Bharti, H. N. S. Yadav, and M. Das, "A Review on Rheological Properties of Magnetorheological Fluid for Engineering Components Polishing," *Materials Today. Proceedings* 56 (2022): A6.

23. C. Qian, Y. B. Tian, Z. H. Fan, Z. G. Sun, and Z. Ma, "Investigation on Rheological Characteristics of Magnetorheological Shear Thickening Fluids Mixed with Micro CBN Abrasive Particles," *Smart Materials & Structures* 31 (2022): 095004.

24. Z. H. Fan, Y. B. Tian, Q. Zhou, and C. Shi, "Enhanced Magnetic Abrasive Finishing of Ti–6Al–4V Using Shear Thickening Fluids Additives," *Precision Engineering* 64 (2020): 300.

25. Z. Ma, Y. B. Tian, C. Qian, S. Ahmad, X. F. Ma, and Z. G. Sun, "Modeling and Simulation of Material Removal Characteristics in Magnetorheological Shear Thickening Polishing," *The International Journal, Advanced Manufacturing Technology* 128 (2023): 2319.

26. Y. B. Tian, Z. Ma, S. Ahmad, C. Qian, X. F. Ma, and Z. H. Fan, "Theoretical and Experimental Investigation of Material Removal Rate in Magnetorheological Shear Thickening Polishing of Ti-6Al-4V Alloy," *Journal of Manufacturing Science and Engineering* 60 (2024): 365.

27. A. A.Sidpara and J. K. Jain, "Experimental Investigations into Forces during Magnetorheological Fluid Based Finishing Process," *International Journal of Machine Tools & Manufacture* 51 (2011): 358.

28. V. Ganguly, T. Schmitz, A. Graziano, and H. Yamaguchi, "Force Measurement and Analysis for Magnetic Field–assisted Finishing," *Journal of Manufacturing Science and Engineering* 135 (2013): 041016.

29. P. Kala, P. M. Pandey, G. C. Verma, and V. Sharma, "Understanding Flexible Abrasive Brush Behavior for Double Disk Magnetic Abrasive Finishing Based on Force Signature," *Journal of Manufacturing Processes* 28 (2017): 442.

30. H. Liang, Q. S. Yan, J. S. Pan, B. Luo, J. B. Lu, and X. W. Zhang, "Characteristics of Forces in Plane Polishing Based on the Magnetorheological Effect with Dynamic Magnetic Fields Formed by Rotating Magnetic Poles," *Journal of Testing and Evaluation* 49 (2021): 255.

31. Z. L. Huang, Q. S. Yan, J. S. Pan, Z. J. Chen, and J. B. Lu, "Dynamic Magnetic Field Magnetorheological Finishing with Constant Load and Variable Gap," *Precision Engineering* 86 (2024): 388.

32. P. F. Chen, Y. W. Gao, G. Y. Zhao, Y. G. Zhao, G. X. Zhang, and Y. Yang, "Modeling of Material Removal Mechanism on Free-Form Surface in Magnetic Abrasive Finishing Process," *Precision Engineering* 91 (2024): 507.

33. S. Chen, Y. Weng, and B. Yao, "Material Removal Model for Magnetorheological Polishing considering Shear Thinning and Experimental Verification," *Materials Today. Communications* 38 (2024): 108475.

34. A. Misra, P. M. Pandey, and U. S. Dixit, "Modeling of Material Removal in Ultrasonic Assisted Magnetic Abrasive Finishing Process," *International Journal of Mechanical Sciences* 131 (2017): 853.

35. D. H. Tien, P. T. T. Thoa, N. V. Que, and T. N. Duy, "Developing Material Removal Rate from Polishing Force Modeling via Magnetorheological Finishing Using an Improved Halbach Array with a Slider Crank Mechanism for Ti-6Al-4V Alloy," *Materials Today. Communications* 45 (2025): 112360.

36. C. Qian, Y. B. Tian, S. Ahmad, Z. Ma, L. Li, and Z. H. Fan, "Theoretical and Experimental Investigation on Magnetorheological Shear Thickening Polishing Force Using Multi-Pole Coupling Magnetic Field," *Journal of Materials Processing Technology* 328 (2024): 118414.

37. Y. B. Tian, Z. Ma, X. F. Ma, L. Li, and J. W. Yan, "A Cross-Scale Material Removal Prediction Model for Magnetorheological Shear Thickening Polishing," *Journal of Materials Processing Technology* 332 (2024): 118569.

38. M. Yu, X. Y. Qiao, X. J. Dong, and K. Sun, "Shear Thickening Effect of the Suspensions of Silica Nanoparticles in PEG with Different Particle Size, Concentration, and Shear," *Colloid and Polymer Science* 296 (2018): 1119.

39. J. Guo, C. J. Wang, N. Yu, and C. F. Cheung, *Advanced Finishing Technologies for High Performance Manufacturing* (Springer Nature, 2025).

40. J. R. Lin, R. F. Lu, M. C. Lin, and P. Y. Wang, "Squeeze Film Characteristics of Parallel Circular Disks Lubricated by Ferrofluids with Non-Newtonian Couple Stresses," *Tribology International* 61 (2013): 56.

41. P. Lei, S. H. Xuan, J. Wu, L. F. Bai, and X. L. Gong, "Experiments and Simulations on the Magnetorheology of Magnetic Fluid Based on Fe_3O_4 Hollow Chains," *Langmuir* 35 (2019): 12158.

42. V. Sokolovski, T. F. Tian, J. Ding, and W. H. Li, "Fabrication and Characterisation of Magnetorheological Shear Thickening Fluids," *Frontiers in Materials* 7 (2020): 595100.

43. F. Guo, Z. D. Xu, and J. M. Gu, "Effects of Nano-Fumed Silica and Carbonyl Iron Powder of Different Particle Sizes on the Rheological Properties of Shear Thickening Fluids," *Colloid and Polymer Science* 301 (2023): 539.